Design and experiment study of a semi-active energy-regenerative suspension system

2015 Smart Mater. Struct. 24 015001

(http://iopscience.iop.org/0964-1726/24/1/015001)

IOP Publishing Smart Materials and Structures
Smart Mater. Struct. **24** (2015) 015001 (12pp) doi:10.1088/0964-1726/24/1/015001

Design and experiment study of a semi-active energy-regenerative suspension system

Dehua Shi, Long Chen, Ruochen Wang, Haobin Jiang and Yujie Shen

School of Automobile and Traffic Engineering, Jiangsu University, Zhenjiang, 212013, People's Republic of China

E-mail: chenlong@ujs.edu.cn

Received 3 April 2014, revised 27 May 2014
Accepted for publication 16 June 2014
Published 18 November 2014

Abstract

A new kind of semi-active energy-regenerative suspension system is proposed to recover suspension vibration energy, as well as to reduce the suspension cost and demands for the motor-rated capacity. The system consists of an energy-regenerative damper and a DC-DC converter-based energy-regenerative circuit. The energy-regenerative damper is composed of an electromagnetic linear motor and an adjustable shock absorber with three regulating levels. The linear motor just works as the generator to harvest the suspension vibration energy. The circuit can be used to improve the system's energy-regenerative performance and to continuously regulate the motor's electromagnetic damping force. Therefore, although the motor works as a generator and damps the isolation without an external power source, the motor damping force is controllable. The damping characteristics of the system are studied based on a two degrees of freedom vehicle vibration model. By further analyzing the circuit operation characteristics under different working modes, the double-loop controller is designed to track the desired damping force. The external-loop is a fuzzy controller that offers the desired equivalent damping. The inner-loop controller, on one hand, is used to generate the pulse number and the frequency to control the angle and the rotational speed of the step motor; on the other hand, the inner-loop is used to offer the duty cycle of the energy-regenerative circuit. Simulations and experiments are conducted to validate such a new suspension system. The results show that the semi-active energy-regenerative suspension can improve vehicle ride comfort with the controllable damping characteristics of the linear motor. Meanwhile, it also ensures energy regeneration.

Keywords: energy-regenerative suspension, adjust shock absorber, DC-DC converter, damping characteristics

(Some figures may appear in colour only in the online journal)

1. Introduction

Since a conventional suspension system needs no control and external energy input, it possesses high reliability and simple structure but poor comprehensive performance. Hence, the isolation performance fails to meet the requirements of suspension systems in different road conditions. Meanwhile, vibration energy generated by uneven road inputs is also dissipated as heat by the fluid damping of traditional dampers [1].

Active suspension can significantly improve ride comfort, as well as handling performance. However, its high energy consumption prevents it from being widely used. Therefore, scholars have been conducting research based on the feasibility of vibration energy recovery, and the concept of energy-regenerative active suspension has been proposed. By recycling vibration energy, less energy consumption, and even self-powered control, can be realized [2–4]. There is a wide variety of energy-regenerative active suspension structures. Due to its advantages of fast response, good

controllability and easy energy-regeneration, electromagnetic energy-regenerative suspension has become a research hotspot [5–9]. Nakano *et al* [10] proposed a method to analyze the balance between regenerative energy and consumed energy based on a single electric actuator. By designing the controller feedback gain, good isolation performance with self-powered active vibration control can be achieved. Okada and Harada [11] studied the regenerative control of an electrodynamic actuator. For high-speed motion, the electrical energy is regenerated, while at low speed, an active or passive control algorithm is applied. Kawamoto and Suda *et al* [12, 13] proposed an electromagnetic damper (EMD) system, which consists of a DC motor and the ball screw mechanism; the EMD can be used as passive and active suspensions. The modeling of the EMD is also presented and further validated by experiments. Martins *et al* [14] compared the layouts of the hydraulic and electromagnetic active suspension and proved the capability of the linear permanent magnet actuator for automotive suspension systems. Goldner and Zerigian *et al* [15] used an optimally designed regenerative electromagnetic shock absorber and determined the effectiveness of transforming vehicle vertical vibration energy into electrical energy. An electromagnetic energy-regenerative shock absorber was designed by Gawade *et al* in ref. [16]. The static magnetic analysis of the shock absorber is analyzed, and space limitations are taken into consideration for the designing process. Lei Zuo [17] developed a rack and pinion-based shock absorber and derived its dynamic model with consideration to backlash and friction. The electromagnetic regenerative shock absorber retrofit design is described in ref. [18]. Bench experiments and road tests are performed to validate its performance. In 2013, Lei Zuo *et al* [19] introduced a mechanical motion rectifier (MMR) into the regenerative shock absorber to convert the oscillatory vibration into a unidirectional generator rotation, which improves the energy harvesting efficiency and reduces the impact force caused by oscillation. Energy-regenerative suspension reduces the energy consumption, but the damping force of the electromagnetic active suspension for the isolation is all supplied by the actuator. As a result, the demand for the motor-rated capacity, as well as the cost, is increased. What's more, the reliability and safety of the active suspension will also be degenerated in emergency conditions.

Recently, suspension energy-regenerative technologies have mainly focused on the active suspension. However, studies on semi-active energy-regenerative suspension, which is based on an adjustable shock absorber, have rarely been reported. Semi-active suspension attracts great attention in automotive engineering due to its low cost, small energy consumption and superior isolation performance [20–22]. In 2006, Hitachi exhibited an electromagnetic suspension that is composed of a hydraulic damper and a linear motor. It was different from the Bose electromagnetic suspension system in that it had a spring and hydraulic damper, while the Bose just replaced the spring and damper with a linear motor [23, 24]. Therefore, the Hitachi's system is superior in cost and safety. Meanwhile, it provides a new direction for the study of suspension systems.

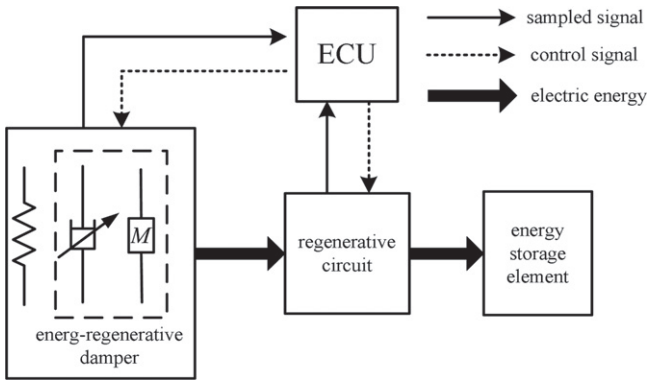

Figure 1. Structural scheme of semi-active energy-regenerative suspension.

Based on the study of the adjustable shock absorber, this paper proposes a new kind of energy-regenerative damper, which is composed of a linear motor and an adjustable shock absorber with three regulating levels; and the linear motor and adjustable shock absorber are in parallel. Furthermore, the sample is trial-produced. When the adjustable shock absorber is at different levels, a different base damping force is achieved. With the adjustable shock absorber providing the different base damping force and the linear motor supplying the continuously controllable electromagnetic damping force, the semi-active energy-regenerative suspension not only has similar isolation performance to that of the active suspension, but it also recovers some vibration energy. Besides, the motor-rated capacity demands and cost are also reduced. A DC-DC converter based on the energy-regenerative circuit is also designed. The double-loop controller has been designed on the basis of analyzing the damping characteristics of semi-active energy-regenerative suspension and the working performance of the energy-regenerative circuit in order to track the desired damping force. At last, simulations and experiments are performed to demonstrate the isolation and energy-regenerative performance of semi-active energy-regenerative suspension.

2. Design of the system

The semi-active energy-regenerative suspension system proposed in this paper is composed of a spring, an energy-regenerative damper, an energy-regenerative circuit and an energy storage element. The energy storage element is just used for storing energy instead of powering the linear motor. Figure 1 shows the structural scheme of a semi-active energy-regenerative suspension system. The system working principle is as follows: The permanent magnet linear motor is driven by suspension vibration; then, part of the vibration energy is converted into electrical energy to charge the energy storage element through the energy-regenerative circuit, and vibration energy recovery is achieved. The induced current interacts with air-gap magnetic field of the permanent magnet, and the electromagnetic damping force is then produced. According to the requirements of energy regeneration and

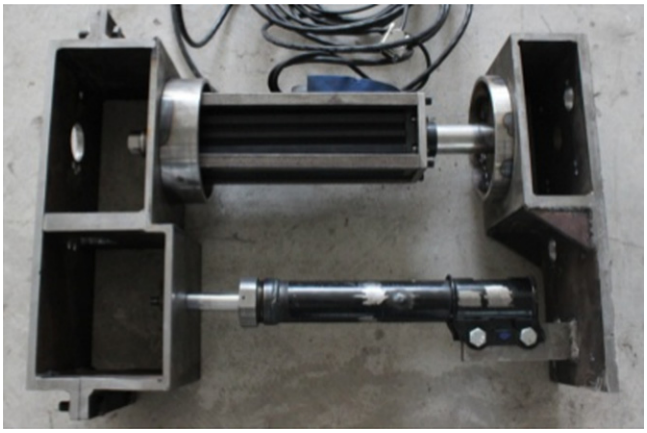

Figure 2. Prototype of energy-regenerative damper.

suspension isolation performance, the shock absorber damping force can be adjusted by regulating the area of the throttling hole, i.e., by regulating the rotation angle of the step motor. The electric motor and the adjustable shock absorber work harmoniously to coordinate the energy-regenerative and damping performance of the semi-active energy-regenerative suspension; in this way, both the improvement of the suspension isolation performance and energy-regeneration is achieved.

2.1. Energy-regenerative damper

The proposed energy-regenerative damper is obtained by integrating a tubular permanent-magnet linear motor into the hydraulic shock absorber with radial orifices in the piston rod. Considering the limitations of individual prototype manufacturing, the prototype is trial-produced by paralleling the linear motor with the adjustable shock absorber, as shown in figure 2. The working principle of the adjustable shock absorber is shown in figure 3. Both the piston rod and the valve are provided with orifices in the radial direction. There are two flowing paths of oil between the two sides of the piston. One path is similar to that of the traditional shock absorber. The oil flows through holes in the piston, as the dashed arrows show in figure 3(a), and the other path passes through the orifices of the piston rod and the valve, as the solid arrows show in figure 3(a). The rotation of the valve is driven by the step motor through a long connecting rod inside of the piston rod. Therefore, the throttling area of the orifices between the piston rod and the valve is regulated by adjusting the step motor rotation angle [25]; the damping is then adjustable. Different working states and the corresponding oil flowing path through the orifices are shown in figure 3(b). There are three damping conditions, such as soft, medium and stiff. When the adjustable shock absorber works in the stiff state, the oil just flows through holes in the piston. While it works in the soft and medium states, different throttling areas of the orifices ensure different damping.

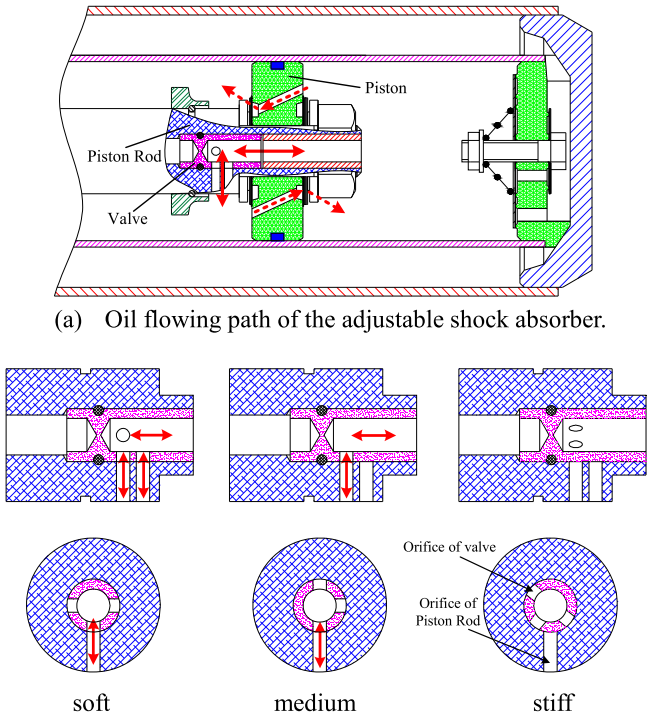

(a) Oil flowing path of the adjustable shock absorber.

(b) Different working states.

Figure 3. Working principle of the adjustable shock absorber.

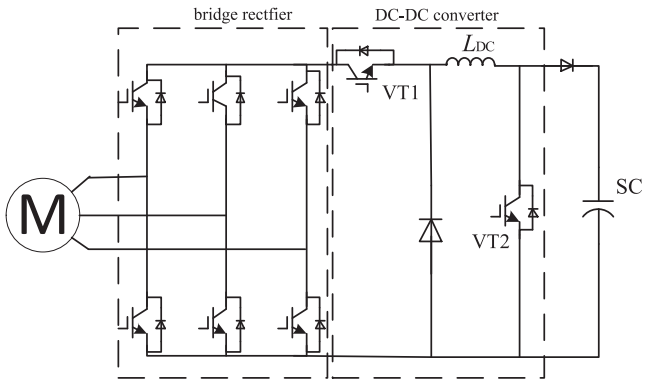

Figure 4. Topology of an energy-regenerative circuit.

2.2. Energy-regenerative circuit

Since the winding is connected with an ultra capacitor or a battery, if the vibration amplitude of the suspension is small, the winding back electromotive force (EMF) may be lower than the voltage of the energy storage element. So, it will lead to poor charging efficiency and damping characteristics of the suspension [11]. In this paper, a modified DC-DC converter is adopted in the circuit, and an ultra capacitor is just used to store energy instead of powering the motor. Figure 4 shows the topology of an energy-regenerative circuit. When a linear motor works as a generator, the induced three-phase AC is transformed into a DC through a bridge rectifier. A DC-DC converter can work in boost and buck modes by means of controlling the power switches VT1 and VT2. When the VT1 switch is on, and the VT2 switch acts as a step-up chopper,

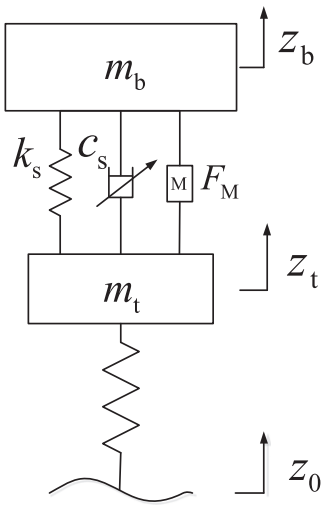

Figure 5. Quarter car model of semi-active energy-regenerative suspension.

the DC-DC converter is in boost mode, and the winding current increases with the duty cycle of the VT2 switch. While the VT2 switch is off, and the VT1 switch acts as a step-down chopper, the DC-DC converter is in buck mode, and the winding current increases with the duty cycle of the VT1 switch.

3. Analysis of the system working characteristics

3.1. Model of the suspension

By simplifying the vehicle into a two degrees of freedom vibration model, the quarter car dynamics model is established, as shown in figure 5, where m_b is the sprung mass, m_t is the unsprung mass, z_b is the sprung mass displacement, z_t is the unsprung mass displacement, k_s is the suspension stiffness, k_t is the tire stiffness, z_0 is the road displacement, c_s is the damping coefficient of the adjustable shock absorber and F_M is the electromagnetic damping force of the linear motor.

According to the model, the kinetic equations are derived as follows:

$$\begin{cases} m_b\ddot{z}_b &= k_s(z_t - z_b) + c_s(\dot{z}_t - \dot{z}_b) + F_M \\ m_t\ddot{z}_t &= -k_s(z_t - z_b) - k_t(z_t - z_0) \\ & \quad -c_s(\dot{z}_t - \dot{z}_b) - F_M \end{cases} \tag{1}$$

In order to suppress the suspension vibration, the electromagnetic damping force provided by the linear the motor, i.e., F_M, is assumed to be

$$F_M = K_i \cdot I \tag{2}$$

where K_i is the linear motor thrust coefficient, and I denotes the motor winding current.

When the linear motor works as a generator, the winding current can be expressed as

$$I = \alpha \cdot I_{max} \tag{3}$$

where α is defined as the current tracking coefficient, and $0 \leqq \alpha \leqq 1$, which indicates the tracking ability of a winding current to the maximum current the linear motor could generate. The maximum current of a linear motor can be written as

$$I_{max} = U_M/R \tag{4}$$

$$\boldsymbol{U}_M = K_e(\dot{z}_b - \dot{z}_t) \tag{5}$$

where U_M is the linear motor back EMF, R denotes the resistance of the linear motor and K_e is the back EMF coefficient of the linear motor.

Let $z_1 = z_b - z_t$, $z_2 = \dot{z}_b$, $z_3 = z_t - z_0$ and $z_4 = \dot{z}_t$, $\boldsymbol{Z} = [z_1 \ z_2 \ z_3 \ z_4]$ is selected as the system state vector, $\boldsymbol{Y} = [\dot{z}_2 \ z_1 \ z_3]$ is selected as the system output vector and $\boldsymbol{U} = [z_0 \ F_M]$ is selected as the system control input vector. Hence, the system state equation can be expressed as follows:

$$\begin{cases} \dot{\boldsymbol{Z}} = \boldsymbol{AZ} + \boldsymbol{BU} \\ \boldsymbol{Y} = \boldsymbol{CZ} + \boldsymbol{DU} \end{cases}$$

where $\boldsymbol{A}$, $\boldsymbol{B}$, $\boldsymbol{C}$ and $\boldsymbol{D}$ are the system state matrix, respectively, which can be obtained by system dynamics equations.

3.2. Damping characteristics

The system damping force includes the fluid damping force of the adjustable shock absorber and the electromagnetic damping force of the linear motor.

The fluid damping force can be expressed as

$$\boldsymbol{F}_s = c_s(\dot{z}_b - \dot{z}_t) \tag{6}$$

where c_s is the fluid damping coefficient.

The electromagnetic damping force is proportional to the winding current and can be written as

$$F_M = \alpha K_i I_{max} = \alpha\frac{K_i K_e}{R}(\dot{z}_b - \dot{z}_t) \tag{7}$$

Let $c_M = \alpha\frac{K_i K_e}{R}$, which can be defined as the electromagnetic damping coefficient of the linear motor; therefore, the overall damping force is obtained below

$$F = \left(F_M + F_S\right) = (c_M + c_S)(\dot{z}_b - \dot{z}_t) \tag{8}$$

We assume that $c_{eq} = c_M + c_s$, where c_{eq} is defined as the equivalent damping coefficient of the energy-regenerative damper. When the current tracking coefficient α varies between 0 and 1, the electromagnetic damping coefficient can be regulated continuously between 0 and K_iK_e/R. Hence, the energy-regenerative damper can be equivalent to a continuously adjustable shock absorber, which has a different base damping c_s and a controllable damping c_M. If a reasonable matching design between base damping c_s and the maximum electromagnetic damping coefficient is conducted, the semi-active energy-regenerative suspension can continuously adjust the damping coefficient in a given range.

By neglecting the asymmetry in the shock absorber jounce and rebound motions, the damping coefficient of the three levels can be defined as c_{soft}, c_{med} and c_{stiff}, respectively, with the damping coefficient being described as the average of the jounce and rebound process. The maximum damping the linear motor could offer is $c_{Mmax} = K_eK_i/R$. Hence, the

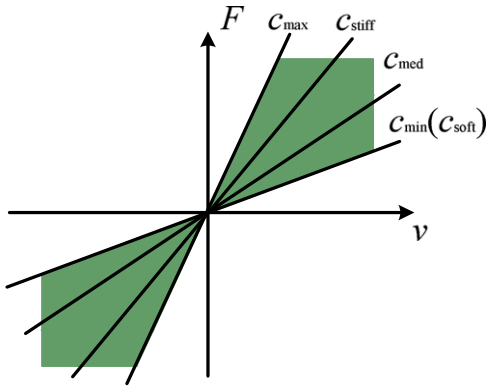

Figure 6. Control bound for semi-active energy-regenerative damper.

passivity-constraint is given by $[c_{min}, c_{max}]$, where $c_{min} = c_{soft}$, and $c_{max} = c_{stiff} + c_{Mmax}$, as shown in figure 6.

3.3. Working characteristics of the circuit

In order to analyze the working characteristics of an energy-regenerative circuit, models under different working conditions of the circuit are established, in which the DC-DC converter is assumed to operate in CCM (continuous conduction mode), and parasitic parameters of the elements in the circuit are ignored [26]. Usually, the capacitance of the ultra capacity is large, and the terminal voltage of the ultra capacity remains nearly constant during the switching period of VT1 and VT2.

3.3.1. Boost mode. When the converter works in boost mode, the VT1 switch is normally on, and the VT2 switch plays the role of the chopper; then, the voltage can be magnified to different degrees by controlling the duty cycle of the VT2 switch.

When the VT2 switch is on, we can get

$$(L + L_{DC})\frac{di}{dt} + iR = U_M \tag{9}$$

When the VT2 switch is off, the circuit relations meet the equation as follows:

$$(L + L_{DC})\frac{di}{dt} + iR + U_C = U_M \tag{10}$$

where L is the inductance of the electric motor winding, L_{DC} is the dynamic inductance, U_C is the terminal voltage of the ultra capacitor and i is the instantaneous value of the electric motor winding current.

According to equations (9) and (10), the transient current response of the winding current can be obtained when the VT2 switch is on or off, respectively. Based on the results, the steady value of the linear motor winding current in a cycle can be derived through approximation by the Taylor series and can be expressed as

$$I = \frac{U_M - (1 - D)U_C}{R} \tag{11}$$

where D is the duty cycle.

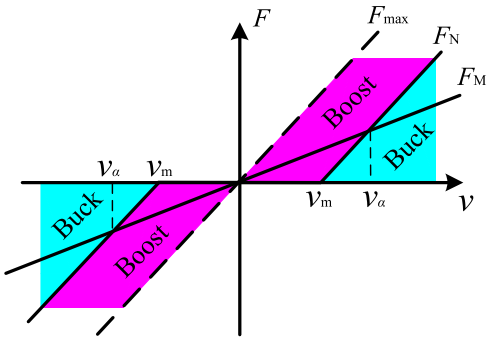

Figure 7. Electromagnetic force of the linear motor with different DC-DC working modes.

3.3.2. Buck mode. When the converter is on buck mode, the VT2 switch is normally off, and the VT1 switch plays the role of the chopper; then, the voltage can be diminished in different degrees by controlling the duty cycle of the VT1 switch.

When the VT1 switch is on, we have

$$(L + L_{DC})\frac{di}{dt} + iR + U_C = U_M \tag{12}$$

When the VT1 switch is off, the winding current is

$$i = 0 \tag{13}$$

When the converter operates in buck mode, if duty cycle D is 1, the ideal maximum winding current could be depicted as

$$I = \frac{U_M - U_C}{R} \tag{14}$$

If duty cycle D equals 0, the minimum winding current is zero. The winding current could be regulated between 0 and $(U_M - U_C)$/R by controlling the duty cycle of VT1 when the converter operates in buck mode. And the regulating range of the winding current in boost mode could be derived from equation (11).

3.4. Operation mode switch basis of the circuit

While the linear motor just works as a generator, the maximum current of winding is limited by the motor working speed. In this case, the maximum electromagnetic damping force produced by the motor can be calculated from

$$F_{max} = K_i\frac{U_M}{R} \tag{15}$$

According to equations (9) to (14), the range of the electromagnetic damping force can be achieved when the DC-DC converter works in different modes, as shown in figure 7. In the figure, v_m ($v_m = U_C/K_e$) is the critical speed to overcome 'dead zone.' The F_N—v curve represents the damping force versus the velocity characteristics when linear motor winding is directly connected to the ultra capacitor. The F_{max}—v curve denotes the maximum damping force versus the velocity characteristics that the motor can theoretically achieve. The F_M—v curve represents the actual damping force versus the

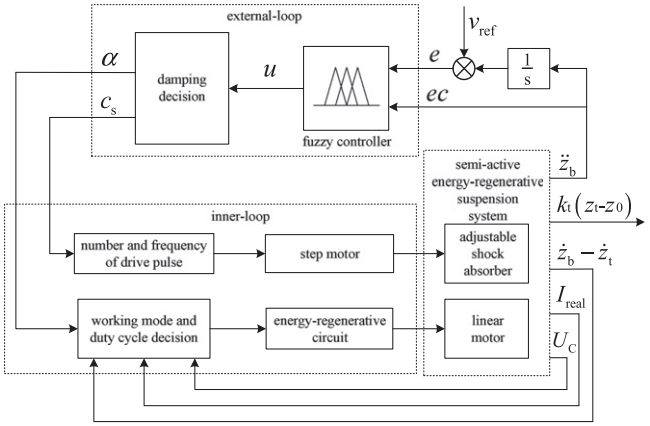

Figure 8. Control system of semi-active energy-regenerative suspension.

velocity characteristics that the motor actually provides. The F_{max}—v curve, F_N—v curve and the v axis form the damping force operation area of the linear motor when the DC-DC converter works in boost mode. The F_N—v curve and the v axis form the damping force operation area in buck mode. v_α is the switching speed for changing the converter operation mode. By changing the converter operation modes and the duty cycle of the VT1 or the VT2 switch, the winding current can be adjusted continuously; that is, the electromagnetic damping force can be adjusted continuously between 0 and F_{max}. It is worth noting that the linear motor with the large thrust force coefficient and the back EMF coefficient, as well as the low resistance, can make the slope of the F_{max}—v curve larger, which means a better isolation performance and energy-regenerative performance of suspension.

According to figure 7, when the motor works at the speed of v_α, the following equation can be derived:

$$\alpha\frac{K_e K_i}{R}v_\alpha = \frac{K_e v_\alpha - U_C}{R}K_i \tag{16}$$

Therefore, in order to track the desired electromagnetic damping force, the following control strategy is designed:

When $v < v_\alpha$, the DC-DC converter works in boost mode, the VT1 switch is normally on and the duty cycle of the VT2 switch is adjusted;

when $v > v_\alpha$, the DC-DC converter works in buck mode, the VT2 switch is normally off and the duty cycle of the VT1 switch is adjusted.

4. Controller design

Comfort and road-holding are two main performance indices of suspension. Improvement in one of the two performance indices often leads to the deterioration of the other [27]. Therefore, the principle of the controller design is to improve comfort without apparently attenuating the road-holding. Then, the double-loop controller is designed for semi-active energy-regenerative suspension. The double-loop includes an external-loop and an inner-loop, as shown in figure 8. The external-loop is a fuzzy controller [28, 29], which produces the controllable force u that the system needs. According to the passivity-constraint and the present relative velocity between the sprung mass and the unsprung mass, c_{eq} can be decided. Then, the base damping c_s and the current tracking coefficient α is determined. Based on the two values, the inner-loop controller offers the pulses for controlling the stepper motor, the decision signals for selecting the operation mode of the energy-regenerative circuit and the duty cycle, with the purpose of making the adjustable shock absorber and the electric motor to produce the ideal damping force.

Table 1. Fuzzy control rules.

u \ e c	NB	NM	NS	ZE	PS	PM	PB
NB	PB	PB	PB	PM	PM	ZE	ZE
NM	PB	PB	PB	PM	PM	ZE	ZE
NS	PM	PM	PM	PM	ZE	NS	NS
ZE	PM	PM	PS	ZE	NS	NM	NM
PS	PS	PS	ZE	NM	NM	NM	NM
PM	ZE	ZE	NM	NB	NB	NB	NB
PB	ZE	ZE	NM	NB	NB	NB	NB

4.1. The external-loop controller

The fuzzy control doesn't depend on the accurate model of the controlled plant. It is decided on the basis of control experience and knowledge, which ensures good robustness. The fuzzy control is used in the external-loop controller. The difference between the actual value and the expected value of the vehicle body vertical velocity is chosen as error signal e. The change rate of e, i.e., body vertical acceleration, is chosen to be error change rate ec. Since the ideal situation is that the vehicle body won't vibrate under random road excitations, the expected value of the vehicle body vertical velocity is set to be zero. e and ec are input variables of the controller external-loop, and controllable force u is the output variable. The basic domain of e is [−0.8, 0.8], and that of ec is [−6, 6]. The fuzzy domains of e and ec are all set to be [−6, 6]. The basic domain of u is [−1500, 1500], while its fuzzy domain is [−6, 6]. {NB, NM, NS, ZE, PS, PM, PB} is chosen as the language value of the input and output variables of the fuzzy controller; the fuzzy control rules are listed in table 1.

4.2. The inner-loop controller

The inner-loop controller is used to regulate the base damping of the adjustable shock absorber and the electromagnetic damping force of the linear motor.

4.2.1. Base damping control of the adjustable shock absorber. The base damping control of the adjustable shock absorber can be changed into the rotation angle control of the stepper motor. The rotation angle of the step motor is adjusted by controlling the frequency and the number of pulse signals. When the pulse frequency is

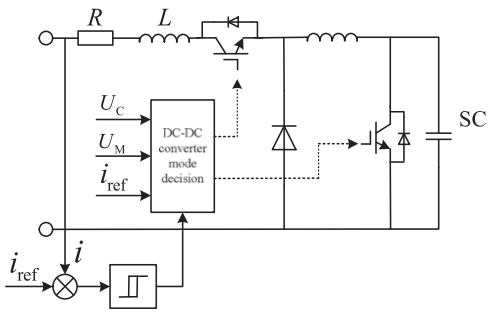

Figure 9. Control block diagram of the energy-regenerative circuit.

changed, the stepper motor rotation speed is changed, and it is also easy to locate the stepper motor by controlling the pulse number. In this way, the desired base damping can be produced by the adjustable shock absorber.

4.2.2. Electromagnetic force control of the linear motor. Since the electromagnetic damping force of the linear motor is associated with the winding current, the control of the electromagnetic damping force can be transformed into the control of the winding current. Figure 9 shows the control block diagram of the energy-regenerative circuit, where i_{ref} is the desired winding current derived from the desired electromagnetic damping force. i denotes the winding actual current. According to the collected signals of the ultra capacitor terminal voltage, the relative velocity between the sprung mass, the unsprung mass and the desired winding current, the operation mode of the DC-DC converter is decided. Furthermore, the difference between the winding desired current and the actual current is used to produce the duty cycle through the hysteresis control algorithm for the control of the energy-regenerative circuit [30].

5. Simulation analysis

The system simulation is conducted in MATLAB/Simulink based on the two degrees of freedom model of the semi-active energy-regenerative suspension. The vehicle driving at 80 km h^{-1} on a C-class road is selected as the simulation input, and the simulation time is 10 s. In order to reflect the impact of the ultra capacitor terminal voltage on the system, the initial terminal voltage of the ultra capacitor is chosen to be 20 V. Table 2 lists the simulation parameters.

Figure 10 indicates the base damping changing history, and figure 11 shows the changes of current tracking coefficient α. It is obvious that the adjustable shock absorber needs to switch among different levels frequently to achieve the desired damping force. Meanwhile, the current tracking coefficient, which reflects the electromagnetic damping force of the linear motor, changes between 0 and 1.

Body vertical acceleration and tire dynamic load are selected as the indices to evaluate ride comfort and road-holding performance, respectively. Figures 12 and 13 demonstrate the responses of the suspension system in the time domain and the frequency domain, respectively. Table 3

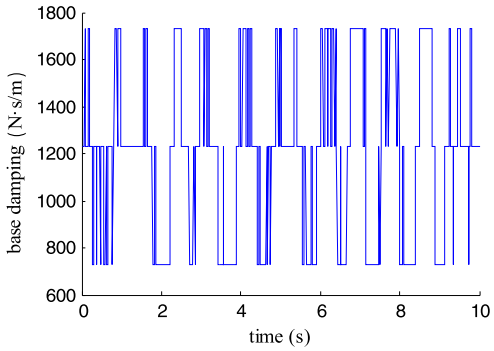

Figure 10. Base damping of the adjustable shock absorber.

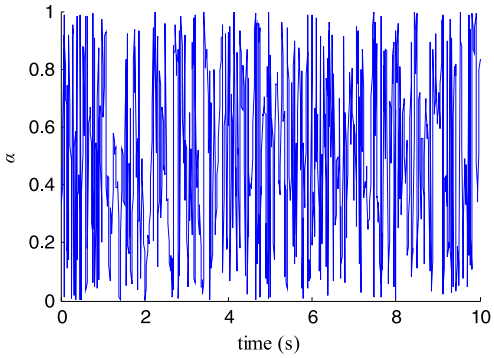

Figure 11. Changing value of α.

Table 2. Simulation parameters.

Parameter	Value
Sprung mass m_b kg^{-1}	317.5
Unsprung mass m_t kg^{-1}	45.4
Suspension stiffness coefficient k_s/(N m^{-1})	22 000
Tire stiffness coefficient k_t/(N m^{-1})	192 000
Base damping coefficient of adjustable shock absorber c_s /(N · s · m^{-1})	730/ 1230/ 1730
Damping coefficient of passive shock absorber c/(N · s m^{-1})	1500
Back EMF coefficient K_E/(V · s m^{-1})	62.6
Thrust force coefficient K_I/(N/A)	77.9
Resistance R/(Ω)	10.16

shows the comparison of the simulation results between the passive suspension and the semi-active energy-regenerative suspension. According to the simulation results, the peak value of the body vertical acceleration and the tire dynamic load are reduced by 10.15% and −0.95%, respectively, and the corresponding RMS values are reduced by 17.24% and −3.41%. This suggests that the ride comfort is improved. Although road-holding performance is degraded, it is acceptable. From figure 13, we can see that the semi-active energy-regenerative suspension provides better ride comfort than the passive suspension at all frequencies, especially around the sprung mass resonance. The reduction is more than 60%. As for road-holding performance, the proposed suspension is superior to passive suspension around the sprung mass

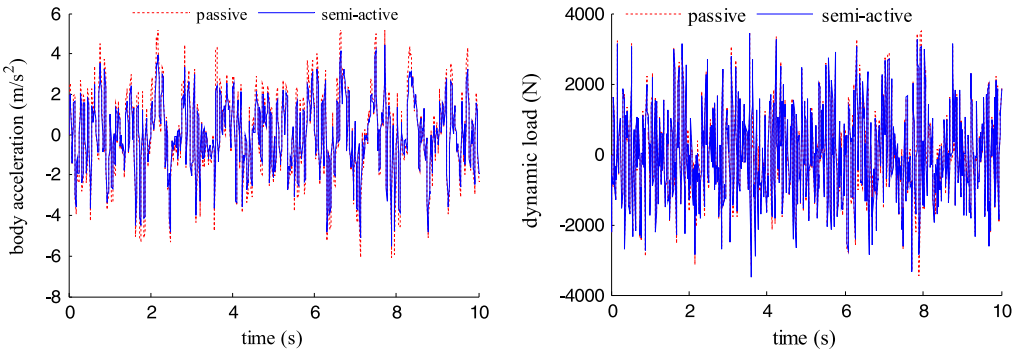

(a) Vehicle body acceleration. (b) Tire dynamic load.

Figure 12. Simulation results of the suspension system in the time domain.

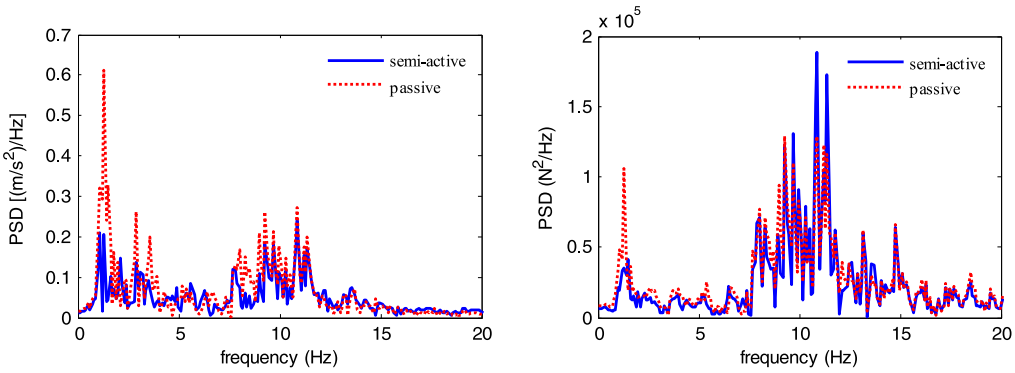

(a) Vehicle body acceleration. (b) Tire dynamic load.

Figure 13. Simulations results of the suspension system in the frequency domain.

Table 3. Comparison of the simulation results.

Performance indices	Semi-active energy-regenerative suspension		Passive suspension	
	Peak value	RMS value	Peak value	RMS value
Body vertical acceleration/ (m s^{-2})	5.468	1.716	6.083	2.073
Tire dynamic load/N	3649.3	1217.0	3528.9	1205.5

resonance. The peak value of the tire dynamic load PSD is sharply reduced at the sprung mass resonance frequency, but around the unsprung mass resonance, the proposed suspension provides a worse result.

Four working cases of semi-active energy-regenerative suspension are compared; they are as follows: in case 1, the designed DC-DC converter is adopted in the energy-regenerative circuit and the controller is as mentioned above. In case 2, the linear motor charges the ultra capacitor directly without the DC-DC converter when the base damping of the adjustable shock absorber is 730 N · s m^{-1}. Cases 3 and 4 are similar to case 2, except that the base damping is 1230 N · s m^{-1} and 1730 N · s m^{-1}, respectively. Figure 14

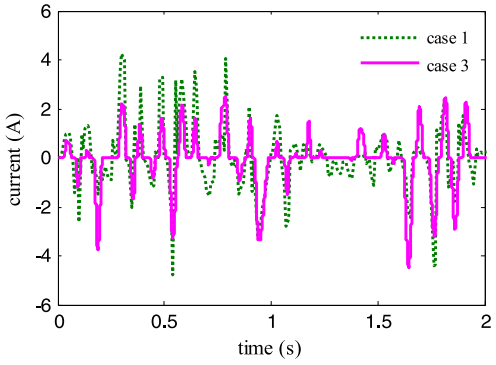

Figure 14. Winging current of linear motor.

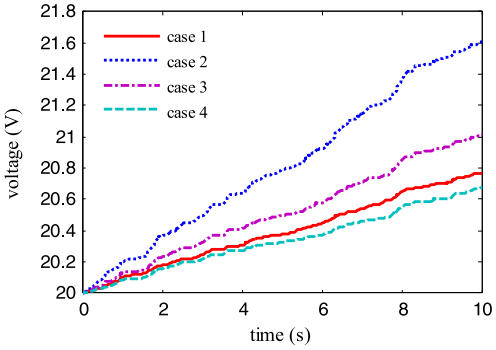

Figure 15. Terminal voltage of the ultra capacitor.

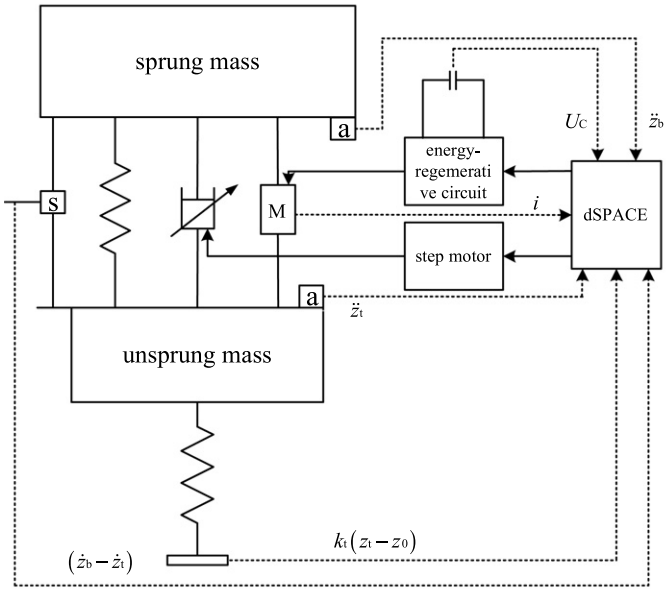

(a) Schematic diagram of experiment set-up.

(b) Bench test physical layout.

Figure 16. Bench test.

shows the changes of winding current, so is the terminal voltage of the ultra capacitor in figure 15 (resistance of ultra capacitor is ignored).

From figure 14, it can be seen that there is no current in the motor windings at some period without DC-DC converter. This is mainly because the vibration amplitude of the suspension system is small, and the winding back EMF is less than the terminal voltage of the ultra capacitor, which leads to the 'dead zone' phenomenon. When the DC-DC converter is adopted and works in boost mode, 'dead zone' can be eliminated.

As observed in figure 15, with the increase of the base damping coefficient, changes in the ultra capacitor terminal voltage slow down, and the energy-regenerative performance is degraded. This is because the larger the base damping, the more energy is dissipated in heat form. As a result, the energy that can be recycled is reduced. Besides, the resistance of the electric motor is large, and a great part of the vibration energy is consumed by the linear motor resistance. In the light of these simulation results, up to 49.89% of the electrical energy produced by the linear motor is consumed by resistance. Therefore, finding ways to reduce the resistance of the linear motor and to improve the recovery efficiency of vibration energy have become key challenges of semi-active energy-regenerative suspension that need to be met.

6. Bench test

Comparative tests between semi-active energy-regenerative suspension and passive suspension are carried out in an INSTRON 8800 CNC hydraulic servo vibration testing machine; the principle of the bench test setup is represented in figure 16. Tire stiffness is simulated by four springs. Two acceleration sensors are used to obtain the acceleration signals of the sprung mass and unsprung mass, respectively. A displacement sensor is used for obtaining the dynamic deflection between the sprung mass and unsprung mass; and through further differential processes, the relative speed between the sprung mass and unsprung mass can be acquired. The current sensor is used to collect current signals, while the voltage sensor is used to capture the terminal voltage of the ultra capacitor. All of the collected signals feed back to dSPACE, which acts as the rapid control prototyping.

The test input is set as random road excitations. The ultra capacitor consists of 12 simple capacitances connected in the series. Each capacity of the capacitances is 100 F, and the ultra capacitor's initial voltage is 20 V. Limited by the test conditions, the test parameters are slightly different from the simulation parameters, but this has no effect on the analysis of the system performance. The results of the bench test are shown in figures 17 and 18 and in table 4.

According to the experimental results, compared with the passive suspension, the ride comfort is improved when the frequency is lower than the unsprung mass resonance frequency. Also, around the sprung mass resonance, the reduction is even more than 50%. The RMS value of the vehicle body vertical acceleration is reduced by 15.31%. However, the tire dynamic load is increased by 2.47%. The reason is that even though the road-holding performance of the sprung mass resonance is improved by the semi-active energy-regenerative suspension, road-holding performance around the unsprung mass resonance is degraded. The conclusions derived from the simulation results and the experimental results match well. The results show that the ride comfort of a semi-active energy-regenerative suspension is improved at the cost of road-holding performance, but the attenuation of the road-holding performance is within acceptable range.

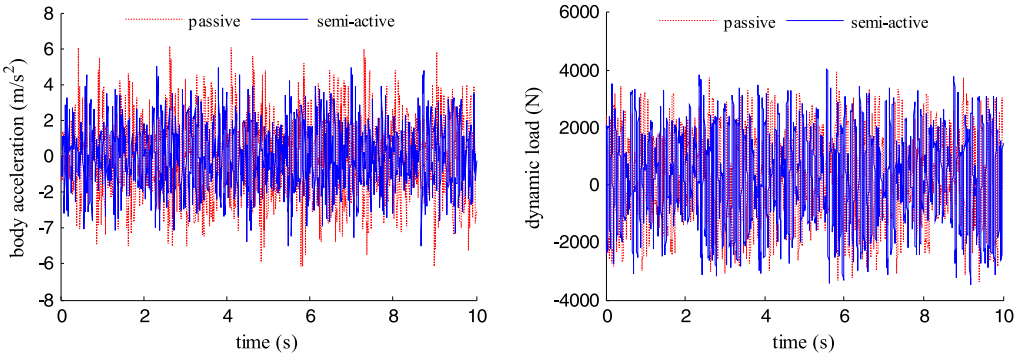

(a) Vehicle body acceleration. (b) Tire dynamic load.

Figure 17. Experimental results of the suspension system in the time domain.

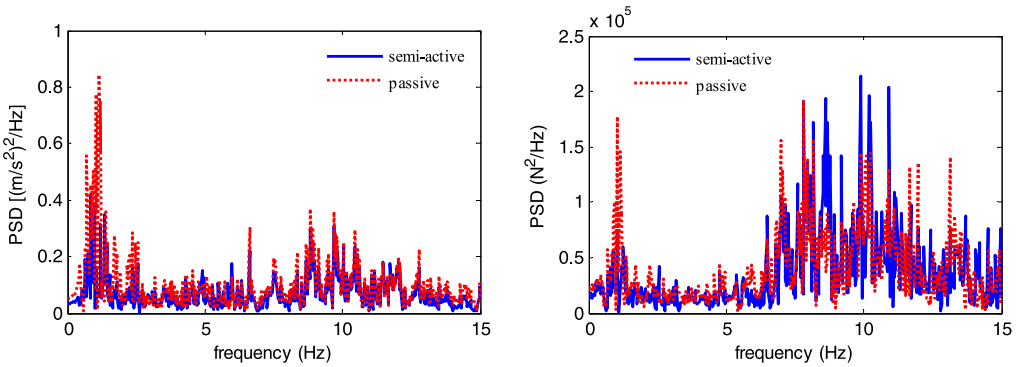

(a) Vehicle body acceleration. (b) Tire dynamic load.

Figure 18. Experimental results of the suspension system in the frequency domain.

Table 4. RMS value of the experimental results.

Performance index	Semi-active energy-regenerative suspension	Passive suspension
Body vertical acceleration/(m s^{-2})	1.680	1.985
Tire dynamic load/N	1360.2	1327.4

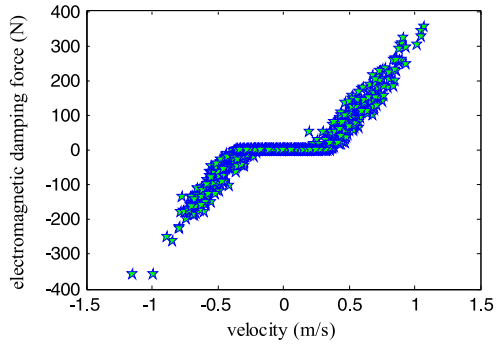

Figure 19. Electromagnetic damping force versus velocity when the linear motor charges the ultra capacitor directly.

When the linear motor directly charges the ultra capacitor in parallel with the 1230 N · s m^{-1} level, the damping force versus the relative velocity characteristic is shown, as seen in figure 19. There are regions where the damping force equals zero, which is called 'dead zone.' Also, when the velocity is large enough to overcome the dead zone, the damping force is proportional to the relative velocity. With the designed energy-regenerative circuit, even though the linear motor just works as a generator, the motor damping force can be adjusted in a certain region under control, instead of displaying a linear characteristic with 'dead zone' phenomenon, as figure 19 shows. The characteristic of the electromagnetic damping force versus velocity with the DC-DC converter is shown in figure 20.

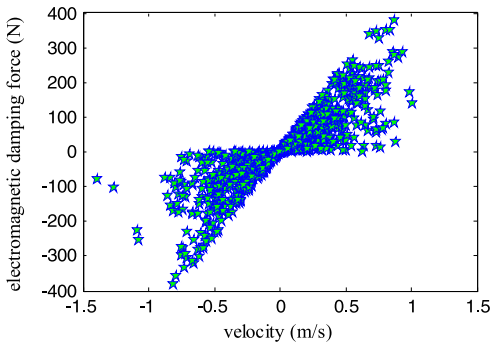

Figure 20. Electromagnetic damping force versus velocity with the DC-DC converter between the motor and the ultra capacitor.

Figure 21 shows the dissipated power by passive suspension P_{passive} and the proposed suspension $P_{\text{semi-active}}$, respectively, as computed from the damping coefficient and

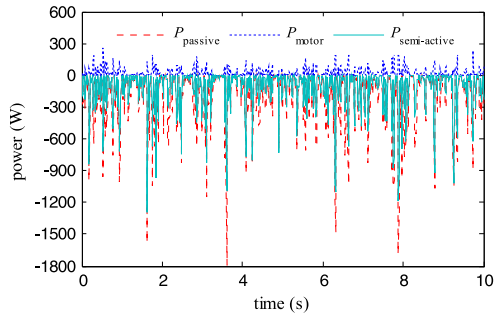

Figure 21. Energy dissipation of the passive suspension and the semi-active energy-regenerative suspension.

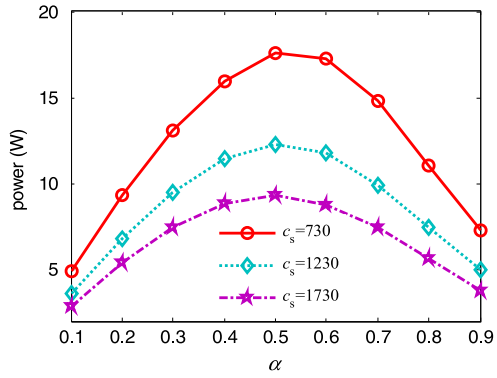

Figure 22. Energy-regenerative power under different control strategies with different base damping.

the relative velocity, along with the power P_{motor} that the linear motor could generate, as computed from the winding current and the relative velocity. When the damping coefficient of the passive suspension equals $1500\,\mathrm{N\cdot s\,m^{-1}}$, the RMS value of the dissipated power is 321.16 W. Under the aforementioned double-loop control, the RMS value of the power dissipated by the adjustable shock absorber of the proposed suspension system is 227.13 W, while the power that the linear motor could generate is 46.57 W. It is obvious that only a small part of the vibration energy is generated by the motor. The reason for this is that the linear motor has a relative low capacity and high resistance. Its maximum electromagnetic damping coefficient, namely K_iK_e/R, is limited. After being multiplied by α, the motor energy-regenerative performance is further degraded.

Figure 22 shows the energy-regenerative power (stored in the ultra capacitor) under different control strategies with different base damping. It can be observed that when the base damping of the adjustable shock absorber increases, the energy-regenerative power decreases, which is consistent with the aforementioned simulation results. With the increase of current tracking coefficient α, energy-regenerative power increases first, then it decreases. The reason is that when α is small, the electromagnetic damping force is small, and the generated power by linear motor is limited; so, the energy-regenerative power is small. When α becomes large, the DC-DC converter works mainly in boost mode. In boost mode, the larger α is, the larger the duty cycle D is. This means that the less time the ultra capacitor is charged. Take $\alpha = 1$ for example; in this case, the largest electromagnetic damping force is obtained when the ultra capacitor is short-circuited, i.e., there is no current charge in the ultra capacitor. All energy generated by the linear motor is dissipated by the winding internal resistance. Theoretically, the energy-regenerative power should be zero. Therefore, when α is large enough, the energy-regenerative power is smaller instead. In fact, under a bench test, the ideal $\alpha = 1$ is difficult to achieve. Due to the control error, there is still slight energy-regenerative power. In this paper, when the fuzzy controller is adopted to improve the suspension system performance, the power stored in the ultra capacitor increases up to 10.13 W. Since the power that the linear motor could produce is 46.57 W, the energy-regenerative efficiency reaches 21.86%, which demonstrates the feasibility of energy regeneration. The other energy generated by the motor is dissipated by internal resistance, copper loss and power loss in the energy-regenerative circuit.

7. Conclusions

In this paper, a new kind of semi-active energy-regenerative suspension based on an adjustable shock absorber and a linear motor is proposed, which reduces the cost and the rated capacity of the actuator, even though, in an emergency, it stills works as a passive suspension. Therefore, the safety is improved. The energy-regenerative circuit based on the DC-DC converter is designed. With the proposed DC-DC converter, the dead zone is eliminated when the motor charges the ultra capacitor, and the motor has controllable damping force versus velocity. A double-loop controller is designed based on the analysis of the damping characteristics of semi-active energy-regenerative suspension and the operating characteristics of an energy-regenerative circuit. Under the control of the double-loop controller, the suspension ride comfort is improved by over 15%, while the road-holding performance is slightly reduced.

Semi-active energy-regenerative suspension could recover a portion of the suspension vibration energy. However, the energy-regenerative power is greatly affected by the damping of the adjustable shock absorber and the wingding resistance. A larger damping coefficient of the adjustable shock absorber and the resistance value mean lower energy-regenerative power. The current tracking coefficient α also has a great effect on the energy-regenerative power; when α approximately equals 0.5, there is the highest power. Meanwhile, since the motor passively damps the suspension vibration, the improvement in both ride-comfort and road-holding performance is limited. Thus, the following study will focus on the active control of the linear motor and its coordination with the adjustable shock absorber to further improve the ride comfort, as well as the road-holding performance, on the basis of energy balance analysis between regenerated energy and consumed energy.

Acknowledgments

It is gratefully acknowledged that this research is financially supported by the National Natural Science Foundation of China (Grant No.50905078) and the Natural Science Foundation of Jiangsu Province (BK 2012714). The authors also express great gratitude for the help of the energy-regenerative suspension research team.

References

[1] Miller L R 1988 Tuning passive, semi-active, and fully active suspension systems *Proc. 27th IEEE Conf. on Decision and Control* pp 2047–53
[2] Nakano K *et al* 2003 Application of combined type self-powered active suspensions to rubber-tired vehicles *JSAE Annual Congress* **6** 19–22
[3] Hsu P 1996 Power recovery property of electrical active suspension systems *Proc. 31st Conf. IEEE Energy Conversion Engineering* vol 3 pp 1899–904
[4] Zuo L and Zhang P S 2013 Energy harvesting, ride comfort, and road handling of regenerative vehicle suspensions *J. Vib. Acoust.* **135** 011002
[5] Jolly M R and Margolis D L 1997 Regenerative systems for vibration control *J. Vib. Acoust.* **119** 208–15
[6] Gysen B L J *et al* 2011 Efficiency of a regenerative direct-drive electromagnetic active suspension *IEEE Trans. Veh. Technol.* **60** 1384–93
[7] Fodor M G and Redfield R 1993 The variable linear transmission for regenerative damping in vehicle suspension control *Veh. Syst. Dyn.* **22** 1–20
[8] Wendel G R and Stecklein G L 1991 A regenerative active suspension system *SAE Technical Paper* No. 910659
[9] Snamina J and Sapiński B 2011 Energy balance in self-powered MR damper-based vibration reduction system *Bulletin of the Polish Academy of Sciences: Technical Sciences* **59** 75–80
[10] Nakano K, Suda Y and Nakadai S 2003 Self-powered active vibration control using a single electric actuator *J. Sound Vib.* **260** 213–35
[11] Okada Y and Harada H 1996 Regenerative control of active vibration damper and suspension systems *Proc. 35th IEEE Conf. on Decision and Control* vol 4 pp 4715–20
[12] Suda Y *et al* 2004 Study on electromagnetic damper for automobiles with nonlinear damping force characteristics: (road test and theoretical analysis) *Veh. Syst. Dyn.* **41** 637–46
[13] Kawamoto Y *et al* 2007 Modeling of electromagnetic damper for automobile suspension *Journal of System Design and Dynamics* **1** 524–35
[14] Martins I *et al* 2006 Permanent-magnets linear actuators applicability in automobile active suspensions *IEEE Trans. Veh. Technol.* **55** 86–94
[15] Goldner R B, Zerigian P and Hull J R 2001 A preliminary study of energy recovery in vehicles by using regenerative magnetic shock absorbers *SAE Technical Paper* No. 2001-01-2071
[16] Patil R U and Gawade S S 2012 Designand static magnetic analysis of electromagnetic regenerative shock absorber *International Journal of Advanced Engineering Technology* **3** 54–9
[17] Li Z, Brindak Z and Zuo L 2011 Modeling of an electromagnetic vibration energy harvester with motion magnification *ASME International Mechanical Engineering Congress and Exposition* pp 285–93
[18] Li Z *et al* 2013 Electromagnetic regenerative shock absorbers: design, modeling, and road tests *IEEE Trans. Veh. Technol.* **62** 1065–74
[19] Li Z *et al* 2013 Regeneративeshock absorber with a mechanical motion rectifier *Smart Mater. Struct.* **22** 025008
[20] Ivers D E and Miller L R 1989 Experimental comparison of passive, semi-active on/off, and semi-active continuous suspensions *SAE Technical Paper* No. 892484
[21] Alanoly J and Sankar S 1987 A new concept in semi-active vibration isolation *Journal of Mechanisms Transmissions and Automation in Design* **109** 242–7
[22] Liu Y, Matsuhisa H and Utsuno H 2008 Semi-active vibration isolation system with variable stiffness and damping control *J. Sound Vib.* **313** 16–28
[23] Akami Y *et al* 2007 Electromagnetic suspension system *US Patent Application* 10/784960
[24] Jones W D 2005 Easy ride: bose corp. uses speaker technology to give cars adaptive suspension *Spectrum IEEE* **42** 12–4
[25] Jiang H B *et al* 2010 Performance simulation and testing of two-levels-damping adjustable hydraulic shock absorber *Chin. J. Mech. Eng.* **46** 117–22 in chinese
[26] Davoudi A, Jatskevich J and De Rybel T 2006 Numerical state-space average-value modeling of PWM DC-DC converters operating in DCM and CCM *IEEE T Power Electr.* **21** 1003–12
[27] Poussot-Vassal C *et al* 2012 Survey and performance evaluation on some automotive semi-active suspension control methods: a comparative study on a single-corner model *Annual Reviews in Control* **36** 148–60
[28] Ting C S, Li T H S and Kung F C 1995 Design of fuzzy controller for active suspension system *Mechatronics* **5** 365–83
[29] Fang Z *et al* 2011 Semi-active suspension of a full-vehicle model based on double-loop control *Procedia Engineering* **16** 428–37
[30] Perry A G *et al* 2007 A design method for PI-like fuzzy logic controllers for DC–DC converter *IEEE Trans. Ind. Electron.* **54** 2688–96